Collisional-radiative-equilibrium spectroscopic diagnosis of a compressed, optically thick neon plasma

J. P. Apruzese,* P. C. Kepple, K. G. Whitney,† J. Davis, and D. Duston
Plasma Physics Division, Naval Research Laboratory, Washington, D.C. 20375
(Received 9 May 1980; revised manuscript received 9 March 1981)

By self-consistently calculating x-ray spectra from first principles, we have delineated the relationships between the spectrum and the state of compression and heating of a neon plasma in detail. A collisional-radiative model including Stark line profiles is used to determine the highly ionized high-density states of neon. One of our calculated spectra reproduces remarkably well an experimental spectrum obtained from laser implosion by Yaakobi *et al.* and indicates compression conditions significantly different from those obtained assuming the validity of local thermodynamic equilibrium. Implications of our calculations for spectroscopic diagnoses of fusion plasmas are discussed.

I. INTRODUCTION

One of the most widely used techniques to diagnose the properties of transient fusionlike plasmas is to analyze their x-ray emissions. In an example of the use of such methods, Yaakobi *et al.*[1] have measured the K-series emission spectrum from a neon plasma produced by laser implosion of a glass microballoon filled with neon at 8.6 atm pressure. Using a methodology that assumed the ionization conditions of the plasma and that accounted for opacity and Stark broadening of the Lyman-α and Stark broadening of the Lyman-β and Lyman-γ lines, they ascribed a density of 0.26 g/cm^3 (ion density, 7.8×10^{21} cm^{-3}) to the neon emission region. From the measured line intensity ratios $I(\mathrm{Ly}\beta)/I(1s^2\text{-}1s3p)$ and $I(\mathrm{Ly}\alpha)/I(\mathrm{Ly}\beta)$, an electron temperature of 300 eV was inferred in the context of an LTE plasma model whose line radiation was assumed to be a Planck function—saturated. In this paper, we show that a theoretically self-consistent, steady-state analysis of all the main features of such spectra can be carried out that is based on a first-principles calculation in which the only free parameters are the average plasma properties of temperature, density, size, and velocity profile. This analysis leads to a set of general principles governing the relationships of high density, optically thick plasma properties to their emitted spectra. As a specific example of the application of such principles, we demonstrate that our calculations reproduce well the neon experimental spectrum discussed above and lead to a diagnosis of significantly lower density and higher temperature. Furthermore, our investigation allows an exposition of how and why a self-consistent physical model reproduces an experimental spectrum, while a simpler but inappropriate model such as LTE may lead to miscalculation and/or misinterpretation of the spectrum.

II. PLASMA MODEL

For spectrum calculations we have employed a detailed multistate, multilevel model of ionized neon in the context of collisional-radiative equilibrium and an assumed spherical geometry. Since virtually all of the neon at peak compression consists of lithiumlike or more highly stripped ions, the model includes only the ground states for Ne I–Ne VII. For lithiumlike Ne VIII, the atomic model includes the excited states $1s^2$-$2p$, -$3s$, -$3p$, -$3d$, and -$4d$. For heliumlike Ne IX, we have the excited-state manifold $1s2s\,^1S$, $1s2p\,^3P$, $1s2p\,^1P$, and the $n=3$ and $n=4$ singlet states. For Ne X, $n=2$, 3, 4, and 5 as well as $n=1$ are included. All of the lines appearing in the Rochester spectrum (Lyα, β, and γ, Ne IX $1s^2$-$1s3p\,^1P$, $1s^2$-$1s4p\,^1P$, as well as $1s^2$-$1s2p\,^1P$) are calculated by self-consistently solving fully coupled nonlinear radiation transport and rate equations.[2] Most importantly, the calculation also includes the self-consistently computed effects of Doppler, Stark,[3] and mass-motional line broadening. Additionally, the calculated spectra are convolved with 1.5 eV of experimental (Gaussian) broadening.[1] However, in most cases, as pointed out by Yaakobi *et al.*, the experimental broadening has little or no effect due to the large Stark linewidths. The rate equations and the radiative transport equation are also used to solve in detail for the continuum radiation arising from recombination from the bare nucleus to the $n=1$ and 2 states of Ne X, and from Ne X $n=1$ to Ne IX $1s^2\,^1S$ and $1s2p\,^3P$.[2]

With the exception of electron collisional excitation rate coefficients and spontaneous decay rates, the methods of calculating the various rate coefficients used in this study have been described in detail in previous papers,[4,5] and only brief reference will be made to these. Every state is coupled to the next (energetically) highest ground state, by collisional ionization and collisional re-

combination. Additionally, photoionization and radiative recombination are computed in detail for the states mentioned above. The collisional ionization rates are calculated by Seaton's prescription,[6] and the photoionization cross sections are calculated in the hydrogenic approximation[7] using effective free-bound Gaunt factors.[8] Collisional- and total-radiative recombination rates are then calculated as the detailed balance of these. However, the details of the frequency dependence of the hydrogenic photoionization cross sections are replaced by a simpler exponential profile for the recombination process.[2] In addition, adjacent ground states are coupled by dielectronic recombination[9] found by summing capture rates over a manifold of states above the ionization limit which then decay via cascade to the ground state.

Excited levels of a given ion are coupled to the other excited states in the model and to the ground state by electron collisional excitation and deexcitation, and by spontaneous radiative decay. Collisional couplings include forbidden and spin-flip transitions as well as those which are dipole allowed. For Ne X, the Coulomb-Born approximation[10] was used, while a distorted-wave calculation with exchange[11] was used to calculate the coefficients for Ne VIII and Ne IX. Comparisons of these two methods have been made for several transitions in hydrogenlike Al XIII,[12] and excellent agreement was obtained.

As mentioned above, line photon reabsorption is taken into account by solving the radiation transport equation for six selected resonance lines, five of which appear in the published Rochester spectrum[1] (taken by Yaakobi *et al.*) and are generally used as diagnostics for neon- or argon-filled pellet targets. The present model neglects the effect of radiation reabsorption for lines which couple two excited states, even though such lines are optically thick in some of the cases discussed below. This simplification, however, results in no significant error in these cases, where the density is so high that collisional rates coupling excited states vastly exceed radiative rates and thus dominate the cross coupling of these levels. Unless these lines appear in the spectrum to be analyzed, it is not necessary to perform the radiation transport calculations for them. The same principle does not apply for the resonance lines dominating most spectra, where the reduced collision rates and higher radiative rates result in comparable importance for collisions and radiation, or even radiation dominance in the couplings.

Details of the radiation transport and photocoupling calculations are given elsewhere[2,13] and will not be elaborated here. However, an additional feature—the calculation of the effects of the different Doppler shifts caused by the inhomogeneous velocity profile of a plasma implosion on the emitted line profiles—has been included in the radiation transport algorithm. These effects will be fully discussed in an upcoming paper, but in the particular results of this paper it served us mainly to confirm what had been suspected, that even at implosion velocities of 2×10^7 cm sec^{-1},[14] the effects are small due to the large Stark widths of the lines at high density. For lower density plasmas the effects can be quite significant but it is of little concern here.

In the analysis detailed below, spectra calculated for steady-state plasma conditions are used to interpret an experimental, time-integrated spectrum. While this approach may at first seem questionable, it was justified for the cases considered here—short-pulse Nd laser drivers—by Yaakobi *et al.*[15] in their letter on argon-filled glass microballoon experiments. They found from extensive hydrodynamical simulations of spherical target compressions that the most energetic emission of hydrogenlike lines occurs during a 10-psec time interval during which the plasma properties change little, spatially or temporally. These theoretical results, coupled with the fact that our analysis obtains striking agreement with experiment, indicate that this assumption can be productively employed under these conditions to interpret the emission properties of plasma cores under spherical compression.

III. COMPRESSION DIAGNOSTICS WITH CALCULATED SPECTRA

It is widely recognized that pellet compression along a low adiabat is most desirable in achieving maximum density prior to thermonuclear ignition. Hence, a major goal of laser-driven pellet compression experiments is to obtain the highest possible implosive drive while minimizing preheat. Knowledge of the degree to which this goal is met experimentally may be obtained from a variety of techniques, and one of the prime tools available is spectroscopy. For this purpose, one must know the sensitivity of the emitted spectrum to the plasma's density and temperature. Figure 1 presents three neon spectra calculated for a spherical plasma in CRE. They illustrate the evolution of the emitted spectrum as the same mass of neon is progressively compressed to higher densities and lower temperatures (i.e., along lower adiabats). The lower the adiabat, the closer to the top of the figure the spectrum appears. Increased density is primarily reflected in the widening of the lines due both to larger intrinsic Stark widths and possible opacity broadening. This effect has been utilized

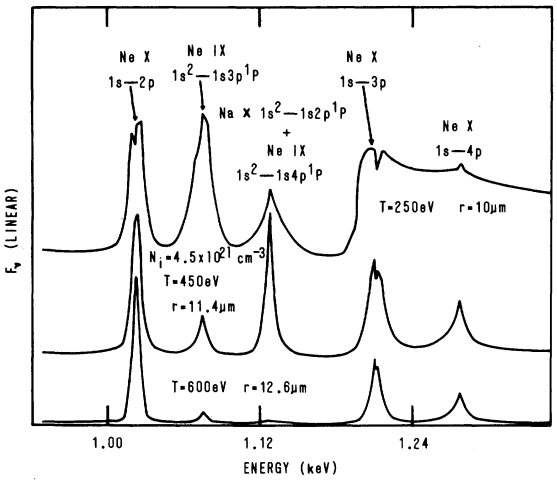

FIG. 1. Three calculated spectra are shown which illustrate, from bottom to top, the changes in spectral signature which occur as a constant neon mass is compressed to higher densities and colder temperatures. The spectra are calculated assuming that the neon plasma is in collisional-radiative equilibrium (CRE). The exterior pellet temperatures decrease from those of the core in accordance with the gradient described in the text. Only the middle spectrum includes the (negligible) pumping effect of the Na x impurity line at 1.13 keV.

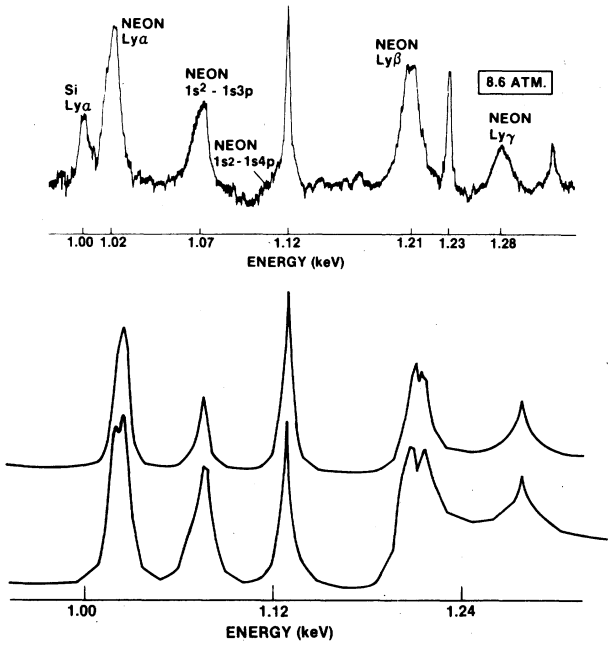

FIG. 2. The top spectrum was obtained by Yaakobi *et al.* at the University of Rochester from a laser-imploded microballoon filled with 8.6 atmospheres of neon. The bottom two spectra were calculated assuming CRE. The middle spectrum provides the best fit to the top one and arises from a plasma of $T_e = 385$ eV, $r = 11.4$ μm at $N_i = 4.5 \times 10^{21}$ cm^{-3}. The bottom spectrum would be emitted by a plasma of $T_e = 300$ eV, $r = 9.5$ μm, at $N_i = 7.8 \times 10^{21}$ cm^{-3}.

for argon compression diagnostics in the case of optically thin nonopacity broadened Stark lines.[16] The line profiles (as opposed to line intensities) are relatively insensitive to temperature.[16] However, effects of opacity broadening are specifically illustrated below in the interpretation of the Rochester neon experimental spectrum[1] taken by Yaakobi *et al.*

The pronounced temperature sensitivity of the emitted spectra is also apparent in Fig. 1. As the temperature is decreased from 600 to 450 to 250 eV, the intensity of the helium-like $1s^2$-$1s3p\ ^1P$ line at 1.074 keV increases dramatically relative to the hydrogen-like Ne X lines. In the Rochester spectrum, the Ne IX $1s^2$-$1s4p\ ^1P$ line (at 1.127 keV) was obscured by the impurity line Na X $1s^2$-$1s2p\ ^1P$, which is equal in wavelength to 1 part in 10^5. In fact this sodium line will optically pump the Ne IX level populations to some degree due to this close resonance. In the middle spectrum of Fig. 1 the effect of this impurity line has been included—the intensity having been derived from our computed fit to the Rochester spectrum[1] (taken by Yaakobi *et al.*) in Fig. 2. We included the sodium pumping line by assuming that the flux directed inward from the microballoon toward the neon filler is the same as the inferred flux directed outward. However, by calculating the emitted neon spectrum without the pumping influence of the impurity line, we have determined that the effect is negligible for these dense plasmas with high collisional cross-coupling rates between excited states. Therefore, the line has been omitted in some of the calculated spectra presented in Figs. 1–3, since its effect on the level populations is negligible.

Equally apparent as the helium line intensity change is the relative increase in the continuum radiation arising from recombination to the ground state of Ne IX as the temperature decreases. Indeed, at a temperature of 250 eV the Lyβ and Lyγ lines which sit on top of this continuum feature (whose edge lies at 1.196 keV) are more properly regarded as "line-continuum features" rather than pure lines. The appearance of this strong continuum edge can place strong constraints on the diagnosed temperature. Also, the continuum opacity may significantly affect both the shape and strength of the observed features arising from bound level transitions. Similarly, ionization by line photons—especially important when the lines are very wide due to Stark effects—may significantly affect the ionization balance of the plasma.

Having noted the spectral differences arising

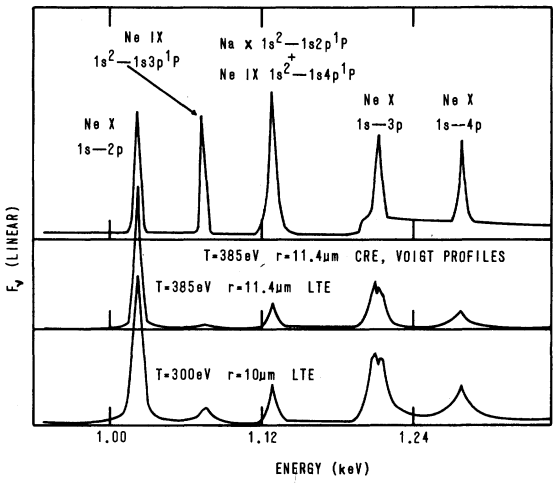

FIG. 3. The three calculated spectra shown represent the results of employing commonly used, but inaccurate, approximations. The top spectrum would be emitted by a neon plasma with pure Voigt line profiles whose conditions are those of the "best fit" of Fig. 2. The middle spectrum maintains the same physical conditions as the top, but Stark line profiles and LTE are assumed. The bottom spectrum arises from the same mass of plasma assumed to be in LTE but with a temperature of 300 eV and a radius of 10 μm. The sodium impurity line at 1.13 keV is included in these spectra.

from changes in density and temperature, we investigated the possibility of obtaining a fit to the Rochester experimental spectrum[1] using our first-principles ionization calculation, in which only temperature, density, size, and velocity variations in plasma conditions could be made.

The results of this effort are graphically summarized in Fig. 2, where the Rochester experimental spectrum (taken from Ref. 1) and two calculated spectra are displayed. The middle spectrum of Fig. 2 represents an excellent fit to the experimental spectrum displayed at the top of the figure. This "best-fit" calculated spectrum would arise from a spherical neon plasma of ion density 4.5×10^{21} cm^{-3} and radius 11.4 μm, having an electron temperature of 385 eV from $r=0$ to $r=8.8$ μm that then decreased smoothly to 296 eV at the surface. This gradient was inferred in a previous analysis of the degree of line self-reversals in such imploded plasmas,[14] and our present results support this gradient inference. Also shown in Fig. 2 (at the bottom) is the spectrum which would be emitted by a neon plasma characterized by the conditions originally inferred from the LTE analysis in Ref. 1. These conditions are $T_e=300$ eV (constant), $N_i=7.8\times10^{21}$ cm^{-3}, and $r=9.5$ μm.

The need for a higher temperature and lower density than previously diagnosed is most readily understood by comparing the predicted 300-eV spectrum to the experimental one. The presence of the prominent continuum feature—the Ne IX ground-state ionization edge—in the 300-eV predicted spectrum is not matched by a similar feature in the experimental one. An explanation for its absence is that the experimental plasma contains less Ne IX and is therefore at a higher temperature, where more of the heliumlike neon is ionized. This degree of reduction of the continuum feature as the temperature increases is clearly evident in the theoretical spectra of Fig. 1, which served as a guide in obtaining the Fig. 2 fit to the Rochester experiment. A core temperature of 385 eV was needed to lower the calculated feature which is weak or nonexistent in the experimental spectrum. Moreover, temperatures higher than 385 eV were found to produce a Ne IX $1s^2$-$1s3p\,^1P$ line which was too weak to match the experimental line. Even at $T=400$ eV, the Fig. 2 comparison of calculated and experimental spectra deteriorated noticeably in this regard. Any temperature below 385 eV raises the helium continuum again producing a significant deterioration in the agreement even at our diagnosed density of 4.5×10^{21}. Our ability to zero in on 385 eV as the likely temperature in this manner strikingly illustrates both the need and the value of utilizing all of the information in the spectrum.

The Rochester analysis yielding $T_e\sim300$ eV was based upon Planckian line ratios generated by an LTE plasma. By contrast we find that a neon plasma of $T_e=300$ eV, $N_i=7.8\times10^{21}$ cm^{-3}, and $r=9.5$ μm has not reached LTE. Of the ionic species, only the Ne X concentration is close to its LTE value. Ne XI (bare nucleus) is about half of what would be expected in LTE, while heliumlike Ne IX has twice its LTE concentration. Moreover, the excited states of Ne X, whose radiative decay dominates the spectrum, are present to a far smaller degree than would be the case in LTE. The LTE excited-to-ground-state ratios of Ne X $n=2$, 3, 4, and 5 are, respectively, 0.13, 0.16, 0.23, and 0.32. We find that the highest ratios occur in the 300-eV model plasma at $r=0$, where they are 0.05, 0.06, 0.09, and 0.13, respectively. In effect, the ionization-excitation state of the plasma lags behind what is required for LTE. At an ion density of 7.8×10^{21} cm^{-3}, collisional processes dominate the coupling of the Ne X excited states to each other. Hence, these ratios of populations of the states lying above $n=2$ to that of $n=2$ do correspond to the required LTE ratios. The Ne X excited states are also in LTE with respect to the ground state lying above (the bare nucleus) due to the strength of collisional ionization and recombination processes. However, collisional excitation from

and de-excitation to the NeX ground state from the excited states is generally at least two orders of magnitude weaker than collisional cross couplings among the excited states. Collisional deexcitation from the excited states to the ground state is also only about one-third as likely as spontaneous radiative decay to the ground state. Collisional processes are therefore not strong enough to enforce LTE between the ground and excited states of the *same* species—NeX. Moreover, due to the large Stark widths, the optical depths of Lyβ, γ, etc., are 2.2 or lower, as described below. Since these modest opacities do not permit multiple photon scattering, the states $n=3$ and above are weakly photoexcited and remain far from LTE with respect to $n=1$. However, since the optical depth of Lyα is ~200, it might at first be suspected that at least $n=2$ would be in LTE with respect to the ground state. The fact that this is not the case may be understood by applying the conditions required for LTE to the rate equations affecting the two states $n=1$ and 2. For simplicity we first consider the two-level-atom case in an optically thick plasma characterized by a line photon escape probability P_e. We let W_{21} stand for the collisional deexcitation rate coefficient and A_{21} stand for the spontaneous emission coefficient. The steady-state condition requires

$$N_2(W_{21}+A_{21}P_e)=N_1\left(W_{21}\frac{g_2}{g_1}e^{-h\nu/kT}\right), \tag{1}$$

where photon reabsorption is accounted for by diluting the spontaneous emission coefficient by a factor equal to the mean photon escape probability. From Eq. (1),

$$\frac{N_2}{N_1}=\frac{(g_2/g_1)e^{-h\nu/kT}}{1+(A_{21}P_e/W_{21})}. \tag{2}$$

For N_2/N_1 to have the LTE population ratio of these two levels, $(g_2/g_1)e^{-h\nu/kT}$, we must have

$$A_{21}P_e \ll W_{21}. \tag{3}$$

Therefore, even a very optically thick plasma can be far out of LTE if $A_{21} \gg W_{21}$ to the extent necessary to offset a small P_e. That is, the mere existence of a small P_e due to large optical depth does not ensure the validity of Eq. (3). Therefore, the fact that Lyα is quite thick in this case does not in itself justify an LTE assumption. For the plasma conditions under consideration here, $A_{21} \cong 2.5W_{21}$. Therefore, LTE will not be valid near the surface of the plasma, where $P_e \approx 0.5$, since $A_{21}P_e \gtrsim W_{21}$ in this region. Of course, the emitted spectrum of optically thick lines tends to be dominated by surface emission. Nevertheless, one still might expect LTE to prevail in the optically thick interior based on the above two-level-atom analysis. However, there are three separate effects which in this case prevent LTE conditions from being established even in the thick plasma interior. First, even though the optical depth of Lyα is ~200, the line wings are so prominent at this high density that the mean escape probability is found numerically to be 0.06. Thus, $A_{21}P_e \cong 0.15\ W_{21}$ in the interior. According to Eq. (2) this alone will reduce the N_2/N_1 ratio to 0.87 times that of LTE. The other two effects which bring the actual ratio to only 0.38 times the LTE ratio are, first, a radiative leak in the Lyβ line, where $\tau \cong 2$, and, second, another photon escape mechanism in the optically grey recombination continuum from the bare nucleus to the ground state of NeX. A multilevel analysis is necessary to clarify the detailed contributions of the latter two mechanisms.

An accurate analytic treatment is possible in this case because the very large collisional rates coupling the excited states ($n=2$, 3, 4, 5, and NeXI) force the ratios of these states to each other to equal those of LTE, as confirmed by the calculated population densities. Let L_{ij} denote the LTE ratio of state i to state j. Then, the equation for the steady-state coupling of NeX $n=1$ to the overlying states becomes

$$N_1\left(\sum_{i=2}^{6} W_{1i}\right)=N_2\Bigg((A_{21}P_{e21}+W_{21}) + \sum_{i=3}^{5} L_{i2}(A_{i1}P_{ei1}+W_{i1}) + L_{62}(W_{R61}N_eP_{e61})\Bigg). \tag{4}$$

In Eq. (4) W_{ij} is the collisional rate coupling states i and j, P_{eij} is the escape probability for the photon emitted during a radiative transition from state i to j, A_{ij} is the spontaneous transition probability, and W_{R61} is the radiative recombination rate from the bare nucleus to NeX $n=1$. Equation (4) contains all of the important processes populating and depopulating NeX $n=1$ at this temperature and density. The processes which are omitted—collisional recombination from NeXI and its inverse, and ionization and recombination processes from and to NeIX—are relatively unimportant compared to what is included, and thus their omission does not quantitatively affect this analysis. Equation (4) is easily solved for N_2/N_1. When the collisional rates and Einstein A's are inserted, the ratio N_2/N_1 is found to be a function of the escape probabilities for a particular plasma temperature, density, and size. For Lyβ, the numerical results yield $P_{e31} \cong 0.7$, and for the $n=1$ recombination continuum $P_{e61} \cong 0.3$. The Lyβ radia-

tion leak in concert with Lyα, γ, and δ would reduce N_2/N_1 to 0.65 times the LTE ratio; inclusion of the free-bound continuum leak brings the ratio down to the actual 0.05, which is 0.38 that of LTE. Photon escape in Lyγ and Lyδ makes little difference since their spontaneous transition probabilities are factors of 4.4 and 13.5, respectively, below that of Lyβ.

In summary, escape of radiation in the optically grey Lyβ and NeXI continuum transitions adds to the radiation escape in the line wings of Lyα and prevents LTE from being established even in the plasma interior. While the strong collisional coupling of the states above NeX $n=1$ forces $n=3$ and above into LTE with $n=2$, it in turn adds to the escape of radiation emitted during decays of these levels and further reduces all the excited-state populations relative to $n=1$. Fundamentally, the lack of detailed balancing of all of the NeX radiation—i.e., by reabsorption—prevents LTE conditions from being established.

The need for a reduced density in order to explain the observed spectrum (from 7.8×10^{21} to 4.5×10^{21} cm^{-3}) is implied by two features of the predicted spectrum at 7.8×10^{21} cm^{-3}; namely, the Lyα, Lyβ, and Lyγ lines are too wide, and the Lyα line exhibits a self-reversal which is not observed. We will first consider the question of the Lyβ and γ lines. As previously mentioned, the total concentration of hydrogenlike NeX in our 300-eV model plasma is roughly equal to the LTE value. However, since our excited-state densities are much less than the LTE amounts, the ground state has a greater than LTE density—varying from 75% greater at the center ($r=0$) to 2.2 times greater at the plasma surface. The reason for this spatial gradient is that the radiation field is less intense at the surface, which therefore, with less optical pumping, contains fewer bare nuclei and more hydrogenlike neon. The optical depths of Lyβ and Lyγ in collisional-radiative equilibrium are therefore about twice the previously assumed LTE values. We find a peak optical depth of 2.2 for Lyβ in contrast to the value of 1.2 that was previously used[1] to calculate the first-order opacity-broadening correction. This results in a 50% increase in linewidth because of the extra opacity broadening. Also, we do not find that the Lyγ line is optically thin; instead, it has a peak optical depth of 1.1. In summary, significantly greater opacity broadening for both Lyβ and Lyγ occurs in CRE than in LTE, which forces a reduction in density in order to reduce the Stark and opacity widths to fit the experimental spectrum.

As noted above, the 300-eV model plasma predicts an asymmetric self-reversal for Lyα. This asymmetry is due to the effects of plasma motion. The self-reversal itself is a well-known effect of large line opacity in a non-LTE plasma. Reducing the linewidth by reducing the density from 7.8×10^{21} to 4.5×10^{21} cm^{-3} turns the self-reversal into a "shoulder" which is more consistent with experiment. The increased temperature of 385 eV reduces the fraction of ground state NeX, and thus the Lyα opacity, contributing to this effect. The width of the opacity-broadened Lyα line is also in very good agreement with experiment when this lower density is assumed, as is apparent in Fig. 2.

IV. EFFECTS OF SIMPLIFYING ASSUMPTIONS ON THE CALCULATED SPECTRA

We have seen above that neither Voigt profiles nor LTE are valid assumptions for the physical state of these high-density neon plasmas. However, it is of interest to invert the analysis and examine spectra calculated using these erroneous assumptions in order to estimate the magnitude of error. Figure 3 displays three spectra which represent the results of employing commonly used, but inaccurate approximations. The top spectrum was computed using conditions identical to those of the "best fit" to the experimental spectrum at the top of Fig. 2, except that Voigt rather than Stark line profiles were used. Consequently, the much narrower lines of this spectrum bear little resemblance to the observed spectrum or to the theoretical Stark-profile spectrum in the middle of Fig. 2. The bottom two spectra of Fig. 3 were computed with Stark profiles but with the LTE assumption. Since the true excitation state of the plasma lags behind LTE, when LTE is assumed, the theoretical excitation state is increased, resulting in more ionization and less NeIX. The reduced heliumlike neon is reflected in the very weak NeIX $1s^2$-$1s3p\,^1P$ line, which for $T=300$ or 385 eV is much less intense than that which is measured. Also, the NeIX ground-state recombination continuum is much reduced, especially in the case of the 300-eV spectrum. Neither LTE spectrum agrees with experiment. It is conceivable that an LTE spectrum of neon at a much lower temperature might show a relatively increased NeIX $1s^2$-$1s3p\,^1P$ line and thus agree more closely with the experimental spectrum of Fig. 2. However, the lower temperature would reduce the collisional rates even further—meaning that LTE would be an even more inappropriate model.

V. SUMMARY AND CONCLUSIONS

We have utilized a first-principles, multistate, multilevel model of highly ionized, high-density neon to predict the emitted spectrum as a function

of the compressed state of the plasma. The appearance of the spectrum has been found to sensitively reflect this state, and the particular features which change in accordance with the various plasma properties have been noted and the underlying physics discussed. The model has been found capable of generating an excellent detailed fit to a previously published experimental spectrum, and the fitting process has led to a considerable refinement of the inferred plasma conditions, including an estimate of the extreme sensitivity of the predicted spectrum to these conditions.

One should note that the authors of Ref. 1 attempted only to obtain an approximate temperature to aid in inferring the density. On the other hand, it is our purpose here to illustrate the potential of non-LTE spectroscopic analysis for obtaining accurate temperatures as well as accurate densities. We have shown that despite the complexity of the dynamics of compression, detailed, realistic, and accurate modeling of the radiative output is both possible and fruitful.

ACKNOWLEDGMENTS

The authors wish to thank Dr. B. Yaakobi for granting permission to use his spectra and for providing a copy for reproduction here. This work was supported in part by the Defense Nuclear Agency.

---

*Science Applications, Inc., McLean, Va.
†Optical Sciences Division.

[1]B. Yaakobi, D. Steel, E. Thorsos, A. Hauer, and B. Perry, Phys. Rev. Lett. 39, 1526 (1977).
[2]K. G. Whitney, J. Davis, and J. P. Apruzese, Phys. Rev. A 22, 2196 (1980).
[3]H. R. Griem, M. Blaha, and P. C. Kepple, Phys. Rev. A 19, 2421 (1979).
[4]D. Duston and J. Davis, Phys. Rev. A 21, 1664 (1980).
[5]K. G. Whitney and J. Davis, J. Appl. Phys. 45, 5294 (1974); J. Davis and K. G. Whitney, *ibid.* 47, 1426 (1976).
[6]M. J. Seaton, Proc. Phys. Soc. London 79, 1105 (1962).
[7]V. L. Jacobs, J. Davis, P. C. Kepple, and M. Blaha, Astrophys. J. 211, 605 (1977).
[8]W. J. Karzas and B. Latter, Astrophys. J. Suppl. Ser. 6, 167 (1961).
[9]V. L. Jacobs and J. Davis, Phys. Rev. A 18, 697 (1978).
[10]L. A. Vainshtein and I. I. Sobel'man, Lebedev Report No. 66 (unpublished).
[11]J. Davis, P. C. Keeple, and M. Blaha, J. Quant. Spectrosc. Radiat. Transfer 16, 1043 (1976).
[12]D. Duston, J. Davis, and K. G. Whitney, NRL Memorandum Report No. 3846 (unpublished).
[13]J. P. Apruzese, J. Davis, and K. G. Whitney, J. Appl. Phys. 48, 667 (1977).
[14]S. Skupsky, University of Rochester Laboratory for Laser Energetics Report No. 80 (unpublished).
[15]B. Yaakobi, S. Skupsky, R. L. McCrory, C. F. Hooper, H. Deckman, P. Bourke, and J. M. Soures, Phys. Rev. Lett. 44, 1072 (1980).
[16]A. Hauer, K. B. Mitchell, D. B. Van Hulsteyn, T. H. Tan, E. J. Linnebur, M. M. Mueller, P. C. Kepple, and H. R. Griem, Phys. Rev. Lett. 45, 1495 (1980).